Examination of Volcanic Activity: AUV and Submersible Observations of Fine-Scale Lava Flow Distributions Along the Southern Mariana Trough Spreading Axis

36

Miho Asada, Shuro Yoshikawa, Nobutatsu Mochizuki, Yoshifumi Nogi, and Kyoko Okino

Abstract

A high-resolution acoustic investigation using the AUV *Urashima* has revealed detailed volcanic and tectonic features along the neo-volcanic zone of the intermediate-rate spreading Southern Mariana Trough, where the high magma flux forms fast-spreading type axial high morphology. Side-scan sonar imagery suggests that the survey area mainly consists of two types of terrain: high-backscattering lumpy terrain occupies the majority of the neo-volcanic zone, and low-backscattering terrain is scattered over the entire area to form various bathymetric features. Visual observations by the submersible *Shinkai 6500* show that the former corresponds to bulbous pillow lava and the latter to jumbled or wrinkled sheet lavas. The estimated proportion of sheet lava with respect to study area is approximately 10 %. Pillow lavas are flatly distributed and do not form the pillow mounds that are common in the slow-spreading Mid-Atlantic Ridge. Furthermore, we did not observe any pillars, collapse features, or axial summit troughs, all of which are frequently reported in the fast-spreading East Pacific Rise.

Keywords

AUV *Urashima* • Low-backscattering terrain • Lumpy terrain • Pillow and sheet lavas • Side-scan sonar

36.1 Introduction

Melt generation and the resulting volcanic activity associated with a seafloor spreading axis generally depend on the spreading rate (e.g., Small 1998; Macdonald 1998). Along back-arc ridges, the correlation between spreading rate and volcanism is more complex owing to the influence of plate subduction processes (Martinez and Taylor 2002; Taylor and Martinez 2003). Taylor and Martinez (2003) systematically analyzed global back-arc basin basalt and proposed that melt generation along back-arc ridges can vary markedly with distance from the volcanic front, mainly due to subduction-induced compositional changes in the mantle rather than the seafloor spreading rate itself. The spreading center of the Southern Mariana Trough shows an axial high morphology similar to fast-spreading ridges, despite its slow to intermediate spreading rate. The back-arc spreading center is very close to the volcanic arc in

M. Asada (✉)
Research and Development Center for Earthquake and Tsunami (CEAT), Japan Agency for Marine-Earth Science and Technology (JAMSTEC), 2-15 Natsushima, Yokosuka, Kanagawa 237-0061, Japan
e-mail: asadam@jamstec.go.jp

S. Yoshikawa
Department of Mathematical Science and Advanced Technology, Japan Agency for Marine-Earth Science and Technology (JAMSTEC), 2-15 Natsushima, Yokosuka, Kanagawa 237-0061, Japan

N. Mochizuki
Priority Organization for Innovation and Excellence, Kumamoto University, Kumamoto, Japan

Y. Nogi
National Institute of Polar Research, 10-3 Midoricho, Tachikawa, Tokyo 190-8518, Japan

K. Okino
Atmosphere and Ocean Research Institute (AORI), the University of Tokyo, 5-1-5 Kashiwanoha, Kashiwa, Chiba 277-8564, Japan

J.-i. Ishibashi et al. (eds.), *Subseafloor Biosphere Linked to Hydrothermal Systems: TAIGA Concept*,
DOI 10.1007/978-4-431-54865-2_36,

this region, although the volcanic front is not clear south of 12°30′N. Previous studies have shown that the magmatic budget increases along the spreading axes in the Southern Mariana Trough because the spreading axis possibly captures heat and melt supply from the volcanic front (e.g., Martinez et al. 2000; Fryer 1996; Taylor and Martinez 2003).

Although previous studies have shown a high magma budget in the Southern Mariana Trough, the style of volcanism (e.g., the distribution of the volcanic product) and lava morphology and texture have not yet been studied. During the TAIGA project, we conducted fine-scale acoustic observations using the AUV *Urashima* and visual observations using the submersible *Shinkai 6500* in the hydrothermal areas of the Southern Mariana Trough (Seama et al., Chap. 17). One of the target areas is the axial zone of back-arc spreading, where it is possible to observe the most recent volcanic activity and active hydrothermal vents. In this chapter, we show the microbathymetry and side-scan sonar imagery collected by the AUV together with photographs taken during the submersible dives. We describe the fine-scale volcanic and tectonic features in the area. This survey gives us the first sub-meter scale observations with ground references along the Southern Mariana Trough, and enables us to obtain a better understanding of volcanism at back-arc spreading centers under the considerable influence of arc volcanism.

36.2 Geological Background

The Mariana Trough is a back-arc basin located behind the Mariana Trench, where the Pacific Plate subducts under the Philippine Sea Plate. The current rate of spreading is approximately 40 mm/year near Guam (13°24′N) (Kato et al. 2003; Martinez et al. 2000) and, based on this spreading rate, the ridge has been categorized as a slow to intermediate spreading ridge.

The spreading axis lies in the eastern part of the basin, indicating asymmetric seafloor accretion (Yamazaki et al. 2003; Deschamps and Fujiwara 2003; Deschamps et al. 2005; Asada et al. 2007). Abyssal hills have not been clearly observed in the eastern off-axis area owing to thick sedimentary coverage and/or overprinting of later arc volcanism (Fryer 1996; Martinez et al. 2000). North of 14°N, the spreading center of the Mariana Trough is morphologically similar to slow-spreading mid-ocean ridges, having a deep crustal graben flanked by a zone of abyssal hills (Seama et al. 2002; Yamazaki et al. 2003), as expected from its slow spreading rate. However, the southern part of the Mariana Trough, where the back-arc spreading axis approaches the volcanic arc (within 10 km at around 13°20′N) (Martinez et al. 2000), shows a broad and smooth morphological cross section and lacks a deep crustal graben (Fig. 36.1). The morphology of this spreading axis is thus similar to that of fast-spreading ridges (Martinez et al. 2000; Martinez and Taylor 2002).

The similarity in morphology to fast-spreading ridges suggests that the spreading ridge of the Southern Mariana Trough receives a considerably higher magma supply than elsewhere along the trough (e.g., Fryer 1996; Martinez et al. 2000; Becker et al. 2010). The highly inflated region along the Southern Mariana Trough is centered at 12°57′N, where the axis forms a broad shallow plateau almost a kilometer wide. The high magma supply in the area is also supported by the existence of a thick crust determined from gravity analysis (Kitada et al. 2006) and by the existence of a melt lens detected by a multi-channel reflection survey (Becker et al. 2010).

Our study area is the neo-volcanic zone of the axial high between 12°56′30″N and 12°57′30″N (Box in Fig. 36.1). The area is the most inflated part along the spreading axis (Martinez et al. 2000; Baker et al. 2005). In the study area, there are two known sites of hydrothermal activity: the Snail site and the Yamanaka site (Fig. 36.2). The Snail site (12°57′12″N, 143°37′12″E) was discovered by an American group using the remotely operated vehicle *Jason* (Wheat et al. 2003). The site is characterized by several high- and low-temperature hydrothermal vents with clear fluid coming up through cracks in outcrops. The Yamanaka site (12°56′42″N, 143°36′48″E) is located approximately a kilometer southwest of the Snail site and was discovered by a Japanese group using the *Shinkai 6500* (Kakegawa et al. 2008). Inactive chimneys and low-temperature simmering have been observed at the Yamanaka site (Kakegawa et al. 2008).

36.3 Data Acquisition

Meter-scale, high-resolution, bathymetric and side-scan sonar data were acquired by the AUV *Urashima* (JAMSTEC), which was built in 1998 (Tsukioka et al. 2005; Kasaya et al. 2011). The AUV *Urashima* is fitted with a 120 kHz side-scan sonar (SSS) for obtaining backscattering intensity data, a 1–6 kHz charp sub-bottom profiler (SBP) for obtaining sub-seafloor sediment information (EdgeTech2200). It is also fitted with a 400 kHz multi-beam echo sounder (MBES) to obtain meter-scale bathymetry data and backscattering intensity data simultaneously (Seabat7125), a depth meter, an altimeter, and a conductivity, temperature, depth, and dissolved oxygen level (CTDO) sensor.

The *Urashima* Dive-91 was conducted at the back-arc spreading center between 12°56′30″N and 12°57′30″N (Fig. 36.2) during the YK09-08 cruise in 2009 (Okino and

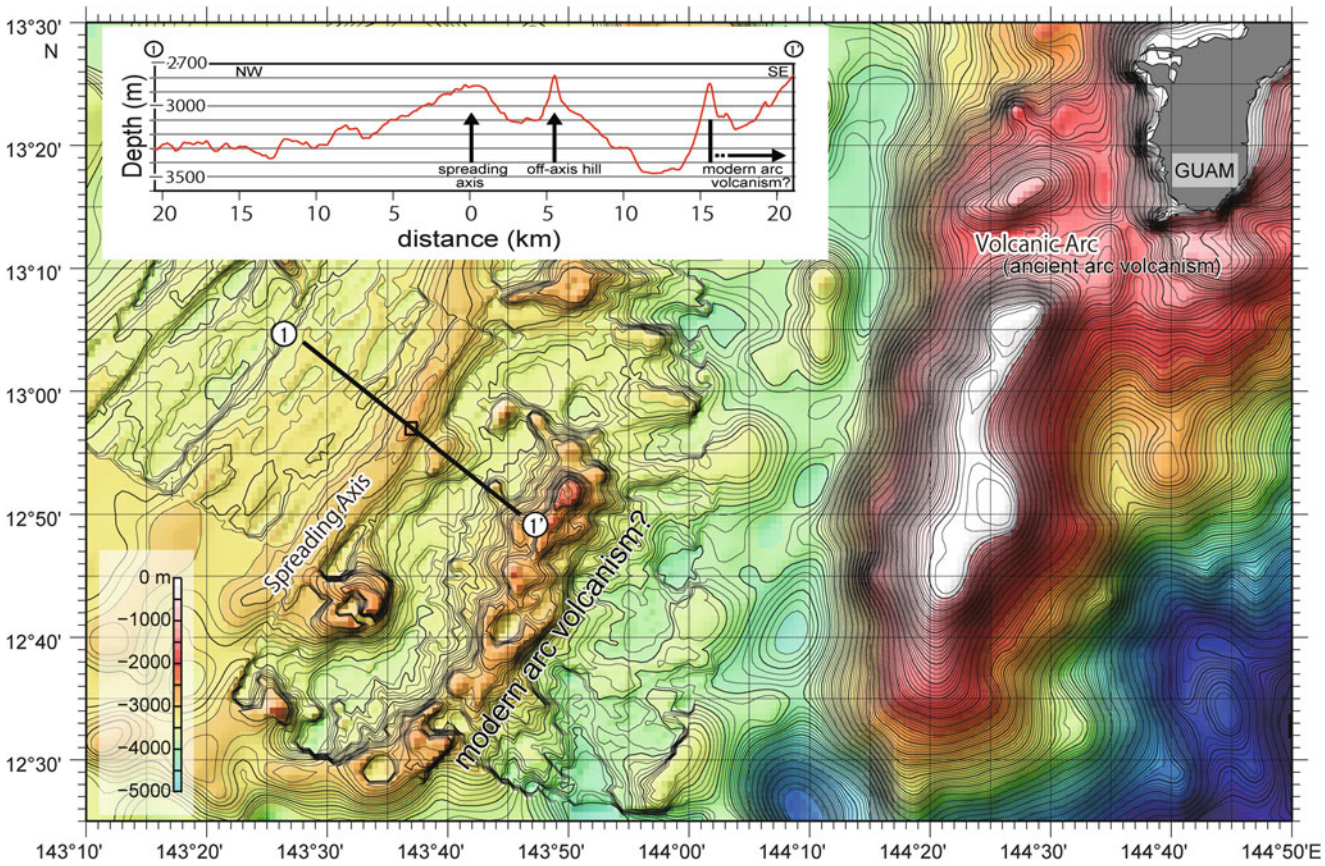

Fig. 36.1 Regional map of the Southern Mariana Trough. The bathymetry data obtained using a *SeaBeam 2112* system on cruise YK09-08 aboard the R/V *Yokosuka* are superimposed on the ETOPO1 dataset (Amante and Eakins 2009). The *box* on transect shows the area shown in Fig. 36.2. The *inset* shows the cross section along the *black line* $1 - 1'$

Shipboard scientific party 2009). The survey was done along seven ~2 km long survey lines parallel to the spreading axis at intervals of roughly 100 m. The obtained data cover an area approximately 2 km long and 1 km wide that includes the neo-volcanic zone. The average survey altitude and speed of the AUV during the YK09-08 cruise were about 100 m and 2 knots, respectively. The expected across-track resolutions for the AUV's acoustic imagery are several meters for the 400 kHz MBES and approximately 7.5 cm for the 120 kHz SSS (when acoustic velocity in seawater is 1,500 m/s). The acoustic beam along-track footprint is 2–5 m (beam width is 0.5° for MBES and 0.9° for SSS). The data processing method is described in Asada et al. (Chap. 37).

In this area, the *Shinkai 6500* submersible performed a total of six dives in 2003 and 2005, and then three more dives after the AUV observation during the YK10-11 cruise in 2010 (Kojima and Shipboard scientific party 2011). We utilized video images and photographs obtained during the dives as ground references for the acoustic imagery data.

36.4 Results and Discussion

36.4.1 Overview of the Survey Area

The micro-bathymetry collected by the AUV-attached 400 kHz multibeam sonar is shown in Fig. 36.2. The northwestern part of the survey area is characterized by well-developed faults; on the contrary, the southeastern part is shallower and dominated by volcanic structures. Hereafter, we refer to these parts as the western and eastern areas following the nomenclature of Yoshikawa et al. (2012) (Fig. 36.2). The mosaic image of the 120 kHz side-scan sonar data and its geological interpretation are shown in Fig. 36.3a and b, respectively.

The western area occupies approximately 30 % of the surveyed area. The side-scan sonar image shows the existence of extensive linear features (Fig. 36.3a, b). These linear features, sometimes associated with acoustic shadows, are generally interpreted as faults, fissures, lava flow channels, and levees. A 30 m high, rectangular hill lies in

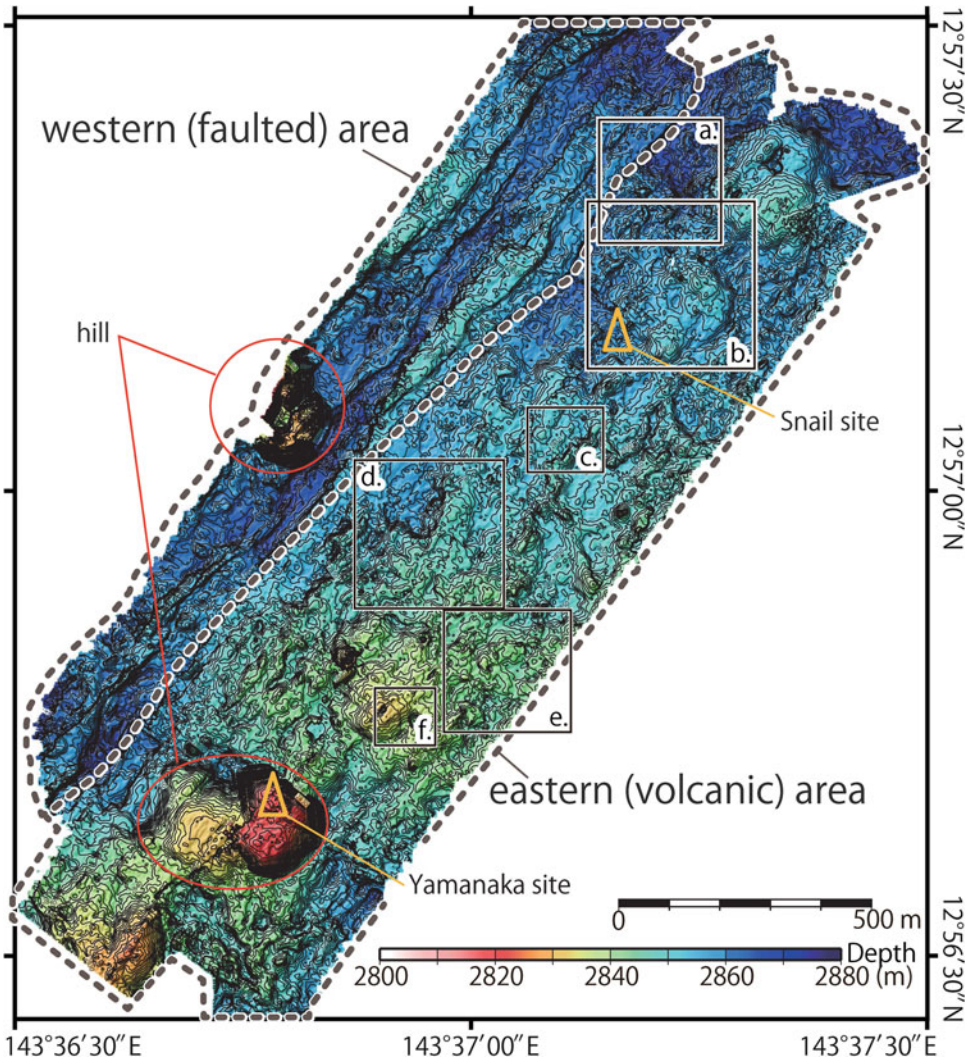

Fig. 36.2 Bathymetry map obtained by the 400 kHz multibeam system mounted on the AUV *Urashima*. Contour interval is 1 m. The enlarged views in *boxes a–f* are shown in Fig. 36.5. *Triangles* indicate the locations of two hydrothermal sites

the area (Fig. 36.2) and is cut by the linear features. The orientation of the linear features is typically NNE–SSW to NE–SW and corresponds well with the orientation of the ridge axis. Both side-scan sonar intensity and SBP data suggest that the sediment cover is very thin or absent in this area.

The eastern area occupies approximately 70 % of the surveyed area. The bathymetry map (Fig. 36.2) shows that this area consists of several mounds, ring-shaped craters, and minor ridges. These volcanic structures are mostly undeformed by faults and are aligned in the NNE–SSW direction, forming the neo-volcanic zone. The relative elevation of these features is 5–10 m. On the side-scan sonar image, we recognize a few linear features that are mostly not associated with acoustic shadows (Fig. 36.3). Generally, such linear features are interpreted as faults or fissures with small vertical throw. Two hydrothermal sites lie in the eastern area (Fig. 36.2). We were unable to recognize any chimney-like structures at and around the Snail site (Fig. 36.4a). A small chimney-like feature was observed on the sonar image at the Yamanaka site (triangle in Fig. 36.4b). The Yamanaka site is situated on an approximately 25 m-high, flat-topped mound (Fig. 36.2), that adjoins another flat-topped mound to the southwest. Other several chimney-like structures were also recognized in between two mounds (circle in Fig. 36.4b). The surface of these mounds corresponds to high backscattering and lumpy terrain (described in the next paragraph) on the sonar imagery. Both side-scan sonar intensity and the SBP data suggest that the sediment cover is very thin or absent in this area, too.

36.4.2 High-Backscattering Lumpy and Smooth Terrains

We categorize the high-backscattering terrain into two groups: lumpy terrain and smooth terrain. Figure 36.5 shows the typical facies of these terrains on the sonar

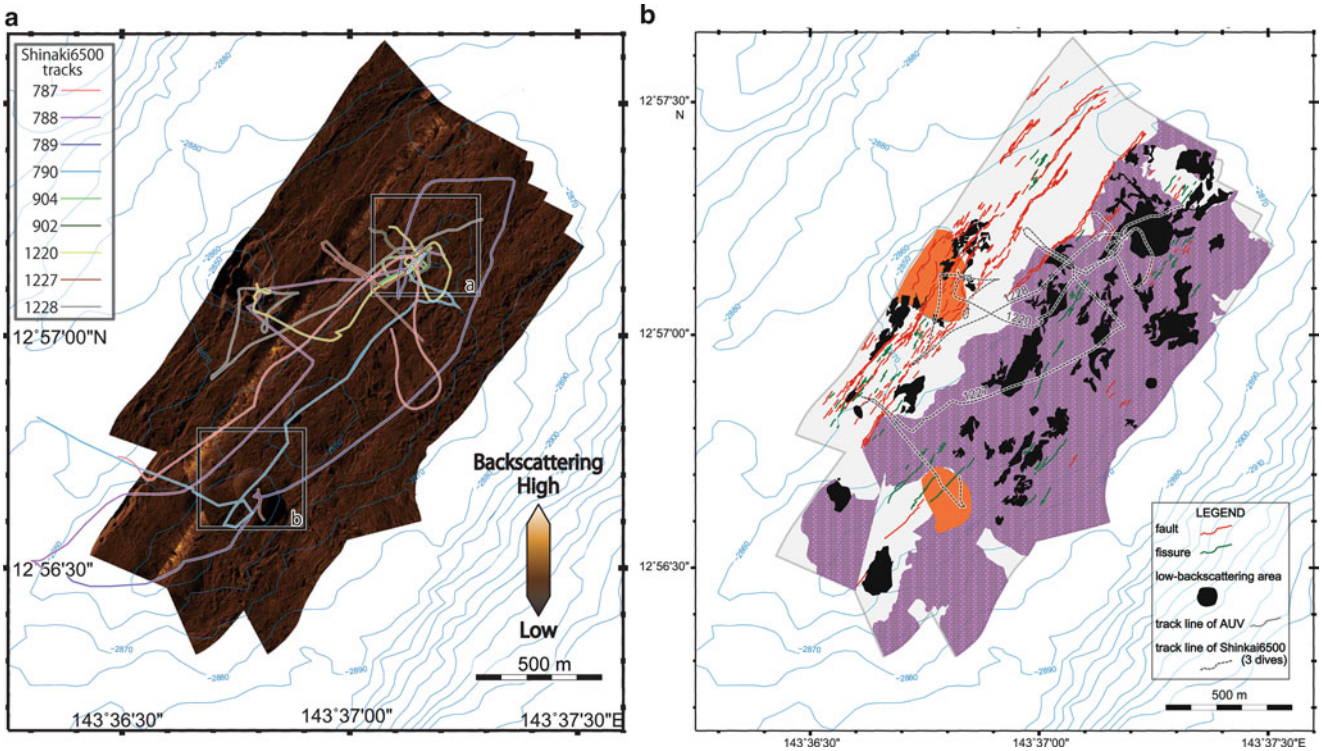

Fig. 36.3 (**a**) Mosaic imagery of 120 kHz side-scan sonar data. *Darker color* indicates lower backscattering intensity. Bathymetry is shown by contours. Tracks of nine submersible dives used for ground reference are indicated. *Boxes a* and *b* indicate the locations of Fig. 36.4a and b, respectively. (**b**) Map showing the interpretation of the side-scan sonar imagery. High-backscattering lumpy terrain and low-backscattering terrain are indicated by *purple* and *black colors*, respectively. *Orange areas* indicate relatively large hills and *gray areas* indicate smooth terrain. *Boxes* indicate the same as in (**a**)

image, and the distribution of these terrains is shown in Fig. 36.3b.

The lumpy terrain is characterized by densely spaced small-scale bumps (lumps) (Figs. 36.5d, g). The typical size of each bump is 20–30 m and the relief is less than a few meters. No dominant direction is recognized for each bump or the distribution pattern. The lumpy terrain occupies most part of the eastern area (Fig. 36.3b).

The smooth terrain is the area exhibiting a smooth surface with finer dots (Figs. 36.5e, h). The terrain shows relatively high backscattering intensity and has no prominent pattern on the sonar image. The smooth terrain covers a large part of the western area (Fig. 36.3b)

36.4.3 Low-Backscattering Terrains

We recognized at least 49 sites of smooth surfaces with low-backscattering signatures on the side-scan image (Fig. 36.3b). These sites, which we refer to as low-backscattering terrain, can be distinguished from the lumpy terrain (Fig. 36.5f, i). The low-backscattering terrain appears as a very fine and homogeneous pattern with few acoustic shadows. The boundaries between the low-backscattering terrain and the lumpy terrain are distinct in some places but ambiguous in others. This variation may be attributed to the differences in age and/or morphological relationships between them. The relative proportion of low-backscattering terrain to lumpy terrain within the observed area was approximately 10 %. The low-backscattering terrains were observed in both the eastern and western areas (Fig. 36.3b). Figure 36.6 shows close up views of the low-backscattering terrains with a sonar intensity profile across these terrains. The low-backscattering terrains are observed in areas with various morphologies: on the top and slope of several mounds, minor ridges, and the slope and bottom of ring-shaped craters.

36.4.4 Visual Observation Using the Manned Submersible, *Shinkai 6500*

The submarine lava shows various surface forms depending on the physical and chemical property of magma, effusion rate, and local surface morphology (Griffiths and Fink 1992; Gregg et al. 1996; Fink and Griffiths 1998; Umino et al. 2000;

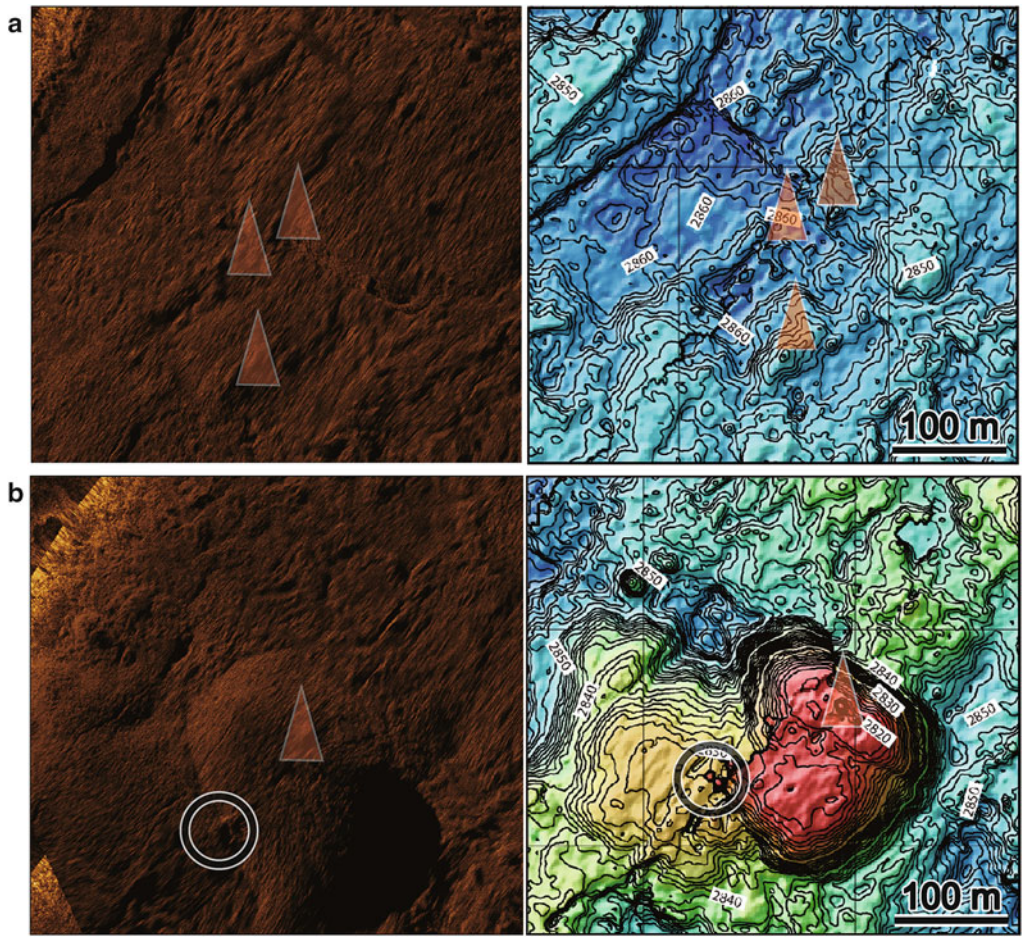

Fig. 36.4 The 120 kHz side-scan sonar images (*left*) and 400 kHz multibeam bathymetry (*right*) of two hydrothermal sites: (*top*) Snail site, (*bottom*) Yamanaka site. The locations of maps are shown by *boxes* in Fig. 36.3a. *Orange triangles* indicate the active hydrothermal areas recognized by visual observation. *Circle* in the *bottom figure* (Yamanaka site) indicate the location at which we recognized a few chimney-like structures on the sonar imagery

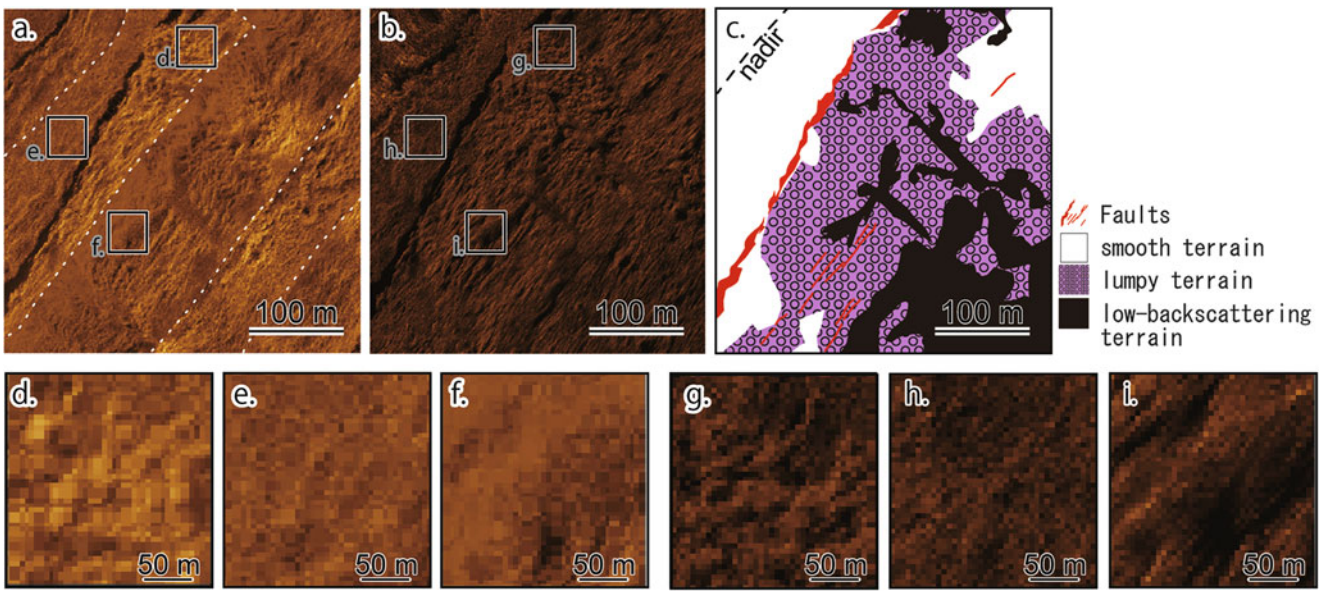

Fig. 36.5 Lumpy, smooth, and low-backscattering terrains on the side-scan sonar image. (**a**) 400 kHz side-scan sonar imagery, (**b**) 120 kHz side-scan sonar imagery, (**c**) interpretation image of the 120 kHz side-scan sonar imagery, (**d**) lumpy terrain (400 kHz), (**e**) smooth terrain (400 kHz), (**f**) low-backscattering terrain (400 kHz), (**g**) lumpy terrain (120 kHz), (**h**) smooth terrain (120 kHz), and (**i**) low-backscattering terrain (120 kHz). *White dotted lines* on the 400 kHz side-scan sonar image indicate the edge of the swath

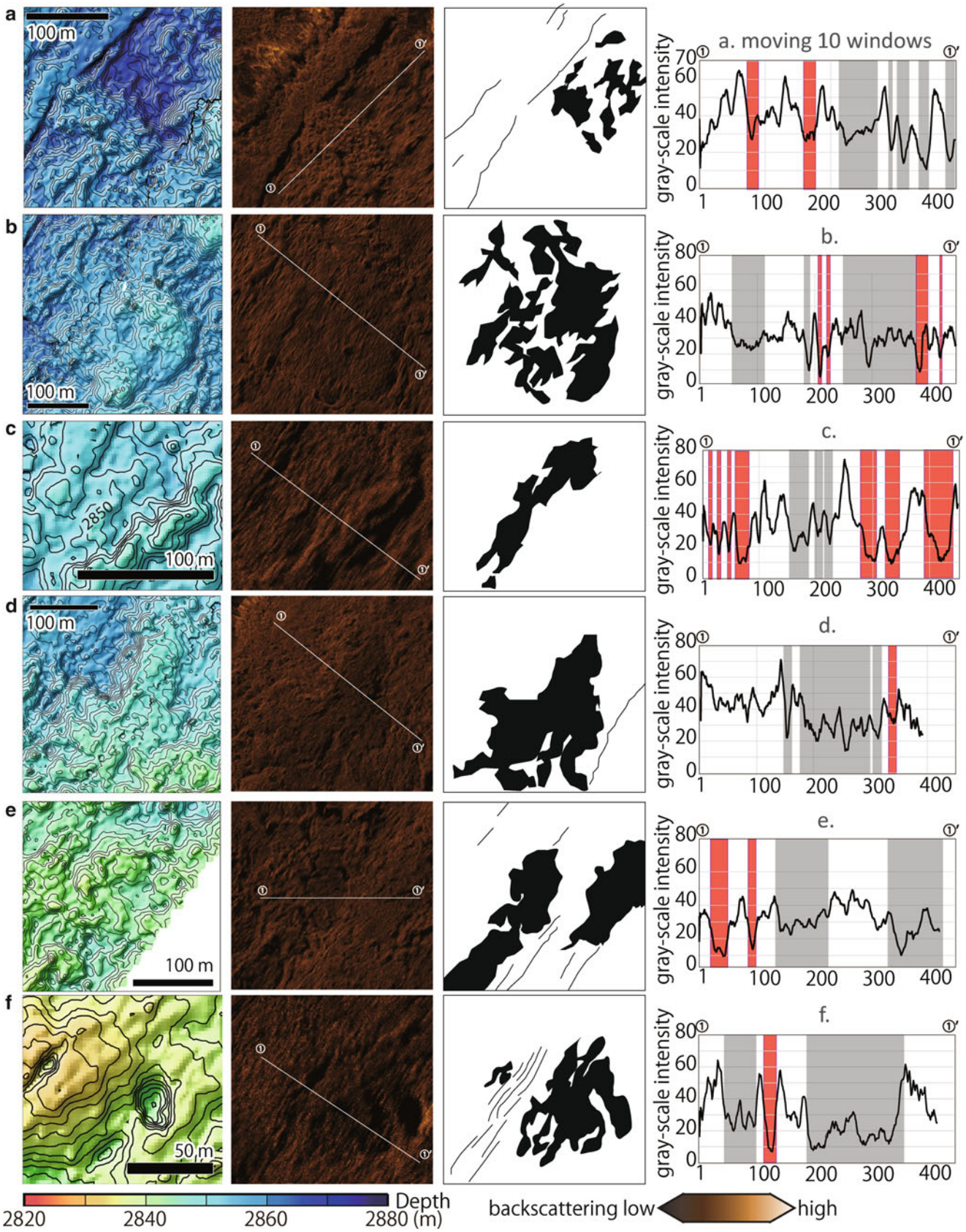

Fig. 36.6 Detailed view of bathymetric features of the low-backscattering terrains. From *left* to *right*, panels show multibeam bathymetry maps, side-scan sonar imagery, interpretation images of side-scan sonar imagery, and intensity along lines shown on the side-scan sonar images. Locations of maps are shown in Fig. 36.2. *Red*- and *gray-colored* areas in graphs indicate the positions of acoustic shadow and low-backscattering terrain, respectively. The *horizontal* and *vertical axes* are pixel number and gray-scale intensity (*darker shades* indicate lower number)

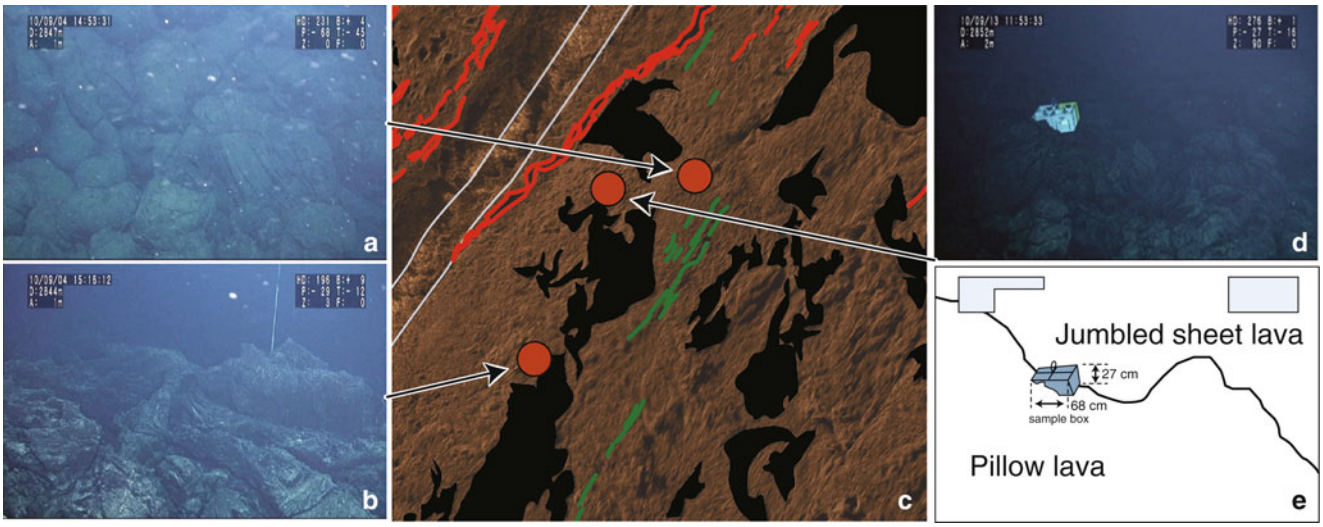

Fig. 36.7 Photos taken by submersible showing a large variety in lava morphology and the corresponding side-scan sonar imagery. (**a**) Photo of pillow lava in lumpy terrain. (**b**) Jumbled sheet lava in low-backscattering terrain. (**c**) Geological interpretation of side-scan sonar imagery. Low-backscattering terrains are shown in *black*. *Red line*, *green line*, and *white line* indicate fault, fissure, and nadir of AUV track and edge of swath, respectively. (**d**) Photo of the boundary of pillow and sheet lava. (**e**) Schematic interpretation of photo (**d**)

Tominaga and Umino 2010). Pillow lavas display bulbous, spherical, or elongate tubular patterns and sheet flows exhibit smooth, lobate, rippled, wrinkled, ropy, whorly, hackly, or jumbled configurations (Fox et al. 1998; Gregg and Fink 1995; Kennish and Lutz 1998; Fundis et al. 2010). Along our observed nine transects of the *Shinkai 6500* dives, the seafloor was mostly covered by bulbous pillow lava with sporadic jumbled, wrinkled, and/or partially fractured (or hackly) types of sheet lava. No axial summit troughs, pillars, or collapse features were observed, even though these features are frequently observed along the fast-spreading East Pacific Rise (Gregg and Chadwick 1996; Gregg and Fornari 1998; Kennish and Lutz 1998; Gregg et al. 2000; White et al. 2002; Haymon and White 2004; Tanaka et al. 2007).

The lumpy terrain on the sonar image corresponds to the flatly distributed bulbous pillow lava (Fig. 36.7a). We found jumbled or wrinkled (and partly hackly) sheet lava in areas consisting of low-backscattering terrains (Fig. 36.7b). We can recognize fragmented pillow lavas in the smooth terrain. We carefully investigated the boundaries between the low-backscattering terrain and the lumpy terrain in the visual records but could not recognize the age difference between theses terrains (Fig. 36.7d, e). Because of the little sedimentary cover over both terrains, differences in backscattering strength likely correspond to differences in the surface morphologies of lava.

Linear features on a hill in the western area (Fig. 36.3b) are faults, which displace the surrounding pillow lavas. Thin sedimentary cover, which was not detected by SBP observations, was observed on the seafloor in the western area. Although turbid water was observed at the foot of the hill, we did not discover any hydrothermal signature in the western area.

Very little sediment was observed in the eastern area. At the Snail site, a hydrothermal plume appeared to be coming up through the cracks of large rocky outcrops, but we did not find any chimney-like structures. The Snail site is located in a valley surrounded by three small mounds. The flat-topped hill on which the Yamanaka site is developed is covered by bulbous pillows at the top and elongated pillows on the slope. These geologic features are consistent with our interpretation of acoustic observations.

36.5 Conclusions

1. We observed the axial zone of the back-arc spreading center in the Southern Mariana Trough using the AUV *Urashima* and the *Shinkai 6500* submersible. The neovolcanic zone is mostly occupied by lumpy terrain with high backscattering intensity. The lumpy terrain consists of flatly distributed pillow lava.
2. Our high-resolution AUV observations using side-scan sonar imagery revealed the existence of low-backscattering signatures. These low-backscattering terrains are associated with a variety of bathymetric features. The submersible observations revealed that the terrain mostly consists of wrinkled and/or jumbled sheet lava, and the edges of the low-backscattering terrains are coincident with the boundaries of pillow and sheet lava types.

3. The proportion of low-backscattering terrain within our observed area is estimated to be approximately 10 %. Since the low-backscattering is interpreted as sheet lava and lumpy/smooth terrains are as bulbous or fractured pillow lavas, the sheet lava occupied ~10 % of seafloor when it is assumed that all of the low-backscattering areas indicate the occurrence of sheet lava.
4. We did not observe axial summit troughs, pillars, or collapse features, all of which are common along the fast spreading East Pacific Rise, in our study area. We also observed a few pillow mounds, which are commonly observed along the intermediate spreading Mid Atlantic Ridge

Acknowledgements We thank the officers and crew of the R/V *Yokosuka*, members of the AUV *Urashima* technical support team, and the scientists onboard the vessel during the YK09-08 and YK10-11 cruises for their help during the collection of the survey data. We appreciate an anonymous reviewer and the editorial board of this e-book for improvement of the manuscript. This research was financially supported by the Ministry of Education, Culture, Science, and Technology (MEXT) of Japan, through a special coordination fund (Project TAIGA: Trans-crustal Advection and In situ biogeochemical processes of Global subseafloor Aquifer, FY 2008–2012).

References

Amante C, Eakins BW (2009) ETOPO1 1 arc-minute global relief model: procedures, data sources and analysis, national geophysical data center, NOAA Technical Memorandum NESDIS NGDC-24, 19 pp, March 2009

Asada M, Deschamps A, Fujiwara T, Nakamura Y (2007) Submarine lava flow emplacement and faulting in the axial valley of two morphologically distinct spreading segments of the mariana back-arc basin from Wadatsumi side-scan sonar images. Geochem Geophys Geosyst 8:Q04001. doi:10.1029/2006GC001418

Baker ET, Massoth GJ, Nakamura K, Embley RW, de Ronde CEJ, Arculus RJ (2005) Hydrothermal activity on near-arc sections of back-arc ridges: results from the Mariana Trough and Lau Basin. Geochem Geophys Geosyst 6:14

Becker NC, Fryer P, Moore GF (2010) Malaguana-Gadao Ridge: identification and implications of a magma chamber reflector in the southern Mariana Trough. Geochem Geophys Geosyst 11:11

Deschamps A, Fujiwara T (2003) Asymmetric accretion along the slow-spreading Mariana Ridge. Geochem Geophys Geosyst 4:8622. doi:10.1029/2003GC000537

Deschamps A, Fujiwara T, Asada M, Montesi L, Gente P (2005) Faulting and volcanism in the axial valley of the slowspreading center of the Mariana back arc basin from Wadatsumi side-scan sonar images. Geochem Geophys Geosyst 6:Q05006. doi:10.1029/2004GC000881

Fink JH, Griffiths R (1998) Morphology, eruption rates, and rheology of lava domes: Insights from laboratory models. J Geophys Res 103:527–545

Fox CG, Murphy KM, Rmble RW (1998) Automated display and statistical analysis of interpreted deep-sea bottom photographs. Mar Geol 78:199–216

Fryer P (1996) Evolution of the Mariana convergent plate margine system. Rev Geophys 34:89–125

Fundis AT, Soule SA, Fornari DJ, Perfit MR (2010) Paving the seafloor: volcanic emplacement processes during the 2005–2006 eruptions at the fast spreading East Pacific Rise, 9 degrees 50′ N. Geochem Geophys Geosyst 11:20. doi:10.1029/2010GC003058

Gregg TKP, Chadwick WW Jr (1996) Submarine lava-flow inflation: a model for the formation of lava pillars. Geology 24:981–984

Gregg TKP, Fink JH (1995) Quantification of submarine lava-flow morphology through analog experiments. Geology 23:73–76

Gregg TKP, Fornari DJ (1998) Long submarine lava flows: observations and results from numerical modeling. J Geophys Res 103:27517–27531

Gregg TKP, Fornari DJ, Perfit MR, Haymon RM, Fink JH (1996) Rapid emplacement of a mid-ocean ridge lava flow on the East Pacific Rise at 9 degrees 46′-51′N. Earth Planet Sci Lett 144:1–7

Gregg TKP, Fornari DJ, Perfit MR, Ridley WI, Kurz MD (2000) Using submarine lava pillars to record mid-ocean ridge eruption dynamics. Earth Planet Sci Lett 178:195–214

Griffiths RW, Fink J (1992) Solidification and morphology of submarine lavas—a dependence on extrusion rate. J Geophys Res 97:19729–19737

Haymon RM, White SM (2004) Fine-scale segmentation of volcanic/hydrothermal systems along fast-spreading ridge crests. Earth Planet Sci Lett 226:367–382

Kakegawa T, Utsumi M, Marumo K (2008) Geochemistry of sulfide chimneys and basement pillow lavas at the Southern Mariana Trough (12.55 degrees N–12.58 degrees N). Res Geol 58:249–266

Kasaya T, Kanamatsu T, Sawa T, Kinoshita M, Tukioka S, Yamamoto F (2011) Acoustic images of the submarine fan system of the northern Kumano basin obtained during the ecperimental dives of the deep sea AUV URASHIMA. Explor Geophys 42:80–87

Kato T, Beavan J, Matsushima T, Kotake Y, Camacho JT, Nakao S (2003) Geodetic evidence of back-arc spreading in the Mariana Trough. Geophys Res Lett 30:1625. doi:10.1029/2002GL016757

Kennish MJ, Lutz RA (1998) Morphology and distribution of lava flows on mid-ocean ridges: a review. Earth Sci Rev 43:63–90

Kitada K, Seama N, Yamazaki T, Nogi Y, Suyehiro K (2006) Distinct regional differences in crustal thickness along the axis of the Mariana Trough, inferred from gravity anomalies. Geochem Geophys Geosyst 7, Q04011. doi:10.1029/2005GC001119

Kojima S, Shipboard Scientific Party (2011) Cruise report on YK10-11 "SHINKAI6500, the southern Mariana Trough". http://www.godac.jamstec.go.jp/catalog/data/doc_catalog/media/YK10-11_all.pdf

Macdonald KC (1998) Linkages between faulting, volcanism, hydrothermal activity and segmentation on fast spreading centers. In: Buck WR, Delaney PT, Karson JA, Lagabrielle Y (eds) Faulting and magmatism at mid-ocean ridges, vol 106. American Geophysical Union, Washington DC

Martinez F, Taylor B (2002) Mantle wedge control on back-arc crustal accretion. Nature 416:417–420

Martinez F, Fryer P, Becker N (2000) Geophysical characteristics of the southern Mariana Trough, 11 deg.50′N-13 deg.40′N. J Geophys Res 105:16591–16607

Okino K, Shipboard Scientific Party (2009) Cruise report on YK09-08 "URASHIMA survey dives". http://www.godac.jamstec.go.jp/catalog/data/doc_catalog/media/YK09-08_all.pdf

Seama N, Yamazaki T, Iwamoto H, Kitada K, Yamamoto M, Fujiwara T, Nogi Y, Okino K, Suyehiro K (2002) Tectonic features of the Mariana Trough, Eos Trans, vol 83, Fall Meet. Suppl., abstract T71F-08, American Geophysical Union, Washington DC

Small C (1998) Global systematics of mid-ocean ridge morphology. In: Buck WR, Delaney PT, Karson JA, Lagabrielle Y (eds) Faulting

and magmatism at mid-ocean ridges, vol 106. American Geophysical Union, Washington DC, pp 1–25

Tanaka A, Rosat S, Kisimoto K, Urabe T (2007) High-resolution bathymetry using Alvin scanning sonar at the Southern East Pacific Rise and its implication to the formation of collapsed lava lakes. Earth Planet Space 59:245–249

Taylor B, Martinez F (2003) Back-arc basin basalt systematic. Earth Planet Sci Lett 210:481–497

Tominaga M, Umino S (2010) Lava deposition history in ODP Hole 1256D: insights from log-based volcanostratigraphy. Geochem Geophys Geosyst 11:19. doi:10.1029/2009GC002933

Tsukioka S, Aoki T, Yoshida H, Hyakudome T, Sawa T, Ishibasi S, Mizuno M, Tahara J, Ishikawa A (2005) The PEM fuel cell system for autonomous underwater vehicles. Mar Tech Soc J 39:56–64

Umino S, Lipman PW, Obata S (2000) Subaqueous lava flow lobes, observed on ROV KAIKO dives off Hawaii. Geology 28:503–506

Wheat CG, Fryer P, Hulme S, Becker N, Curtis A, Moyer C (2003) Hydrothermal venting in the southern most portion of the Mariana backarc spreading center at 12.57°N, EOS Trans, T32A-0920, Fall Meeting 2003. American Geophysical Union, Washinton DC

White SM, Haymon RM, Fornari DJ, Perfit MR, Macdonald KC (2002) Correlation between volcanic and tectonic segmentation of fast-spreading ridges: evidence from volcanic structures and lava flow mrphology on the East Pacific Rise at 9°–10°N. J Geophys Res 107. doi:10.1029/2001JB000571

Yamazaki T, Seama N, Okino K, Kitada K, Joshima M, Oda H, Naka J (2003) spreading process of the northern Mariana Trough: rifting-spreading transition at 22°N. Geochem Geophys Geosyst 4. doi:10.1029/2002GC000492

Yoshikawa S, Okino K, Asada M (2012) Geomorphological variations at hydrothermal sites in the southern Mariana Trough: relationship between hydrothermal activity and topographic characteristics. Mar Geol 303:172–182